Available online at www.sciencedirect.com
SCIENCE DIRECT®
Journal of Solid State Chemistry 177 (2004) 4626–4631
JOURNAL OF SOLID STATE CHEMISTRY
www.elsevier.com/locate/jssc

Syntheses, characterization and electrical property of a new silver diphosphonate with zeolite-like framework and three-dimensional silver interactions: $[Ag_4(O_3PCH_2CH_2PO_3)]$

Ruibiao Fu, Shengqing Xia, Shengchang Xiang, Shengmin Hu, Xintao Wu*

State Key Laboratory of Structural Chemistry, Fujian Institute of Research on the Structure of Matter, Chinese Academy of Science, Number 155, Yanrqiao Road, Fuzhou, Fujian 350002, PR China

Received 5 August 2004; received in revised form 28 September 2004; accepted 5 October 2004

Abstract

A new silver organodiphosphonate, $[Ag_4(O_3PCH_2CH_2PO_3)]$ (**1**), has been synthesized and characterized by X-ray diffraction, IR, TGA-DSC, electricity measurement and element analysis. **1** crystallizes in the monoclinic space group $P2(1)/n$ ($a=6.0115(16)$ Å, $b=8.630(2)$ Å, $c=8.462(2)$ Å, $\beta=97.693(4)^\circ$, $Z=2$, $R_1=0.0604$, $wR_2=0.1450$). **1** contains one-dimensional channels and a three-dimensional Ag···Ag interacted substructural net. TGA and XRD indicate little weight loss up to 300 °C and little structure change after heated at 170 °C for 2 h, respectively. The grain interior conductivity of **1** increases continuously from 50 to 170 °C. Results of EHT calculations show that under thermal or optical excitation the conductivity of **1** is mainly due to transfer of π antibonding electrons of $-PO_3$ group through O atom to Ag 5*s* orbital, which also leads to enhancement of Ag···Ag interactions and promotes formation of Ag···Ag substructural net.

Keywords: Hydrothermal syntheses; Silver; Diphosphonate; Zeolite-like; Single crystal

1. Introduction

Metal organodiphosphonates as new hybrid inorganic–organic materials have attracted a great deal of research interest in the past 10 years, due to many applications as small molecular sensors [1,2], adsorption [3] and catalyst [4]. Particularly, metal organodiphosphonates are very important in preparing meso/microporous materials [5–9] because the open frameworks can be adjusted through modifying lengths and shapes of the organic units. Generally, metal organodiphosphonates are pillar-like structures, such as Cr^{2+} [10], Co^{2+} [11,12], Cu^{2+} [11–14], Zn^{2+} [11,15–17], Al^{3+} [18], Ga^{3+} [19], Ln^{3+} [20], Ti^{4+} [21,22], Zr^{4+} [23–27] and Th^{4+} [28]. However, as far as we know, there are few metal organodiphosphonates with zeolite-like structures in previous work. And only two silver organophosphonates [29,30] and few silver organodiphosphonates have been reported. On the other hand, recently some researches concentrated on understanding of closed shell d^{10} Ag···Ag interactions result in novel supramolecules [31–36] and highly electrical conducting material [37]. This paper describes hydrothermal syntheses, single crystal structure, thermal behavior and electricity property of the new silver organodiphosphonate, which contains a zeolite-like framework and a three-dimensional Ag···Ag interacted substructural net: $[Ag_4(O_3PCH_2CH_2PO_3)]$ (**1**).

2. Experimental

2.1. Generals

1,2-Ethylenediphosphonic acid was prepared according the reported method [38,39]. Other chemicals with

*Corresponding author. Fax: +86 591 371 4946.
E-mail address: wxt@fjirsm.ac.cn (X. Wu).

0022-4596/$ - see front matter © 2004 Elsevier Inc. All rights reserved.
doi:10.1016/j.jssc.2004.10.008

reagent grade quality obtained from commercial sources without further purification. Elemental analysis and infrared spectra were performed with a Vario EL III element analyzer and a Nicolet Magna 750 FT-IR spectrometer, respectively.

2.2. Preparation of $[Ag_4(O_3PCH_2CH_2PO_3)]$ (1)

A mixture of $AgNO_3$ (0.1708 g, 1.005 mmol), $H_2O_3PCH_2CH_2PO_3H_2$ (0.1005 g, 0.5287 mmol), NaF (0.0820 g, 1.95 mmol), H_2O (5.0 mL) and ethanol (5.0 mL) was sealed in 25 ml Teflon-lined stainless steel vessels and heated at 120 °C for 72 h. The role of NaF is increasing pH of reaction through forming HF. After the mixture slowly cooling to ambient temperature, dark yellow needle-like crystals were obtained. The pattern of powder XRD is agreement with that of simulated from single crystal X-ray data, which indicates a homogeneous phase. Yield 0.1091 g (70% based on $AgNO_3$). Elemental analysis for **1**: calcd. for $Ag_4O_6P_2C_2H_4$: C 3.89, H 0.65%. Found: C 3.88, H 0.78%. IR (KBr pellet, cm^{-1}): 3386vs, 2245m, 1674m, 1417w, 1184m, 1107s, 1043s, 958s, 756w.

2.3. Single-crystal and powder X-ray diffraction

X-ray data were collected on a suitable single crystal with dimensions 0.46 mm × 0.06 mm × 0.04 mm at 293 ± 2 K on a Siemens SMART-CCD diffractometer using graphite-monochromated Mo $K\alpha$ radiation (λ(Mo-$K\alpha$) = 0.71073 Å). Data were reduced and absorption corrected with SMART and SADABS software, respectively. The structure was solved by direct methods and refined by full-matrix least-squares techniques on F^2 using SHELXTL-97 [40]. All non-hydrogen atoms were treated anisotropically. The positions of hydrogen atoms were generated geometrically. Details of crystal data and structural refinement for **1** are given in Table 1. Crystallographic data for the structure reported in this paper have been deposited with the Cambridge Crystallographic Data Centre as supplementary publication no. CCDC_246696. Copies of the data can be obtained free of charge on application to CCDC, 12 Union Road, Cambridge CB2 1EZ, UK (fax: (44) 1223 336-033; e-mail: deposit@ccdc.cam.ac.uk). Powder X-ray diffraction (XRD) pattern was acquired on a DMAX-2500 diffractometer using Cu $K\alpha$ radiation.

2.4. Thermal analysis

Thermogravimetric analyses (TGA) and differential scanning calorimetry (DSC) were carried out on a NETZSCH STA 449C unit at a heating rate of 5 °C under nitrogen gas flow from 30 to 800 °C.

Table 1
Crystal data and structural refinement for compound **1**

Empirical formula	$Ag_4O_6P_2C_2H_4$
Formula weight	617.47
CCDC number	246696
Crystal appearance	Dark yellow needle
Crystal size/mm	0.46 × 0.06 × 0.04
Temperature/K	293(2)
Crystal system	Monoclinic
Space group	$P2(1)/n$
a/Å	6.0115(16)
b/Å	8.630(2)
c/Å	8.462(2)
β/deg	97.693(4)
V/Å^3	435.1(2)
Z	2
D calcd./g cm^{-3}	4.713
Diffractometer	Siemens Smart CCD
λ(Mo $K\alpha$)/Å	0.71073
Absorption coefficient/mm^{-1}	9.231
θ for data collection	3.39–25.08
H k l range	−7–4, −10–8, −10–8
Correction	SADABS
Max/min transmission	1.000000/0.583771
F(000)	564
Reflections measured/independent	1238/768 [R(int) = 0.0328]
Observed reflections[$I > 2\sigma(I)$]	651
Refinement method	Full matrix least squares on F^2
Parameter/restraints/data	64/0/651
Goodness-of-fit on F^2	1.196
Final R indices [$I > 2\sigma(I)$]	$R_1 = 0.0604$, w$R_2 = 0.1450$
R indices (all data)	$R_1 = 0.0762$, w$R_2 = 0.1615$
Largest difference peak and hole/e A^{-3}	1.686, −2.140
Software	SHELXTL-97

2.5. Electrical property measurement

Electrical conductivity measurements were performed on complex impedance spectroscopy with an Agilent 4284A precision LCR meter. A pellet of polycrystalline about 4.5 mm diameter and 0.5 mm thickness was prepared by a 709YP-15A powder tablet press at room temperature. Silver electrodes on two faces of the pellet were obtained by application of KD-II Room-temperature Fast-drying Electrically Conductive Adhesive. The pellet was heated at 90 °C for an hour before tested. The measurements were carried out with temperature increasing (50 → 170 °C) and then decreasing (170 → 50 °C) processes with 10 °C interval in an Electric Thermo-static Drier, which controlled by an AI-708P Programmed Automation Regulator. The frequency range for measurements was 20–10^6 Hz.

3. Results and discussion

3.1. Thermal property

As shown in Fig. 1, TGA and DSC of **1** under nitrogen gas flow reveals that there is little weight loss

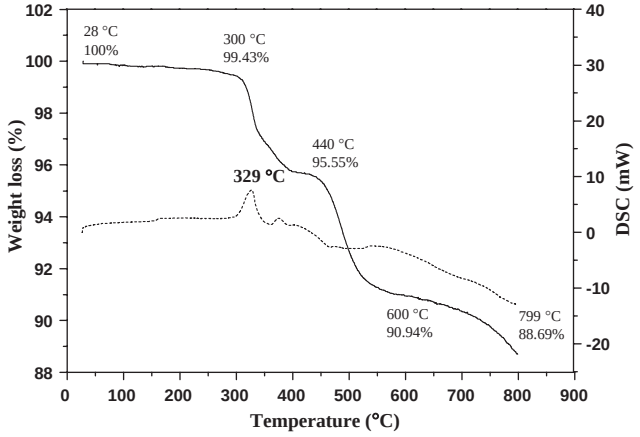

Fig. 1. TGA (solid line) and DSC (dot line) curves of **1**.

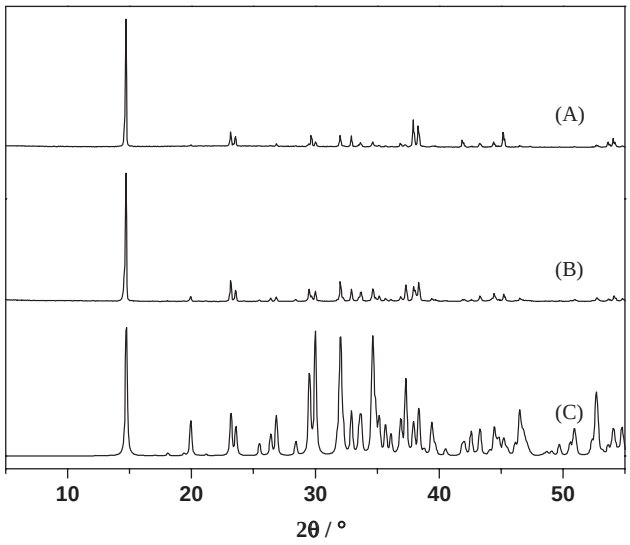

Fig. 2. Powder XRD patterns of **1**: (A) polycrystalline after heated at 170 °C for 2 h under air atmosphere, (B) polycrystalline and (C) simulated from single crystal X-ray data.

up to 300 °C and a decomposing centered at 329 °C, respectively. The total weight loss from 300 to 440 °C is 3.88% (calculated loss of ethylene group = 4.54%). Following that, two continuous weight loss stages are in the temperature range of 440–600 °C and 600–799 °C with 4.61% (calculated loss of 1/3 PO_4 = 5.07%) and 2.25% mass losses, respectively. Polycrystalline of **1** was heated at a heating rate of 0.4 °C min^{-1} from room temperature to 170 °C in an Electric Thermo-static Drier and held at 170 °C for 2 h in air atmosphere. After cooling to room temperature, powder XRD pattern is agreement with that simulated from single crystal X-ray data, which indicates little structure change (Fig. 2).

3.2. Crystal structure description

The asymmetric unit of **1** contains two crystallographically distinct Ag(I) atoms (Fig. 3a). Ag1(I) and Ag2(I) atoms are in distorted tetrahedron [$Ag1O_4$] and triangle [$Ag2O_3$] coordination geometry, respectively. Each oxygen atoms of [$Ag1O_4$] and [$Ag2O_3$] are from different 1,2-ethylenediphosphonate groups with Ag1–O and Ag2–O bond lengths in range of 2.305(12)–2.530(11) Å and 2.203(12)–2.380(11) Å, respectively. [$Ag1O_4$] tetrahedron shares a corner with [$Ag2O_3$] triangle through one oxygen atom (O2). On the other hand, each [PO_3] of 1,2-ethylendiphosphonate group coordinate to seven Ag(I) atoms through two μ_3–O (O2*c* and O3*g*) and one μ_4–O (O2). As a result, the distances of Ag1⋯Ag2, Ag1⋯Ag1*b*, Ag1⋯Ag2*c* and Ag2⋯Ag2*e* are 3.214(2), 3.063(3), 3.223(2) and 3.173(3) Å, respectively, which are shorter than the sum of van der Waals radii of two silver atoms (3.44 Å) [41], indicating four Ag⋯Ag interactions [32,33].

It is interesting that four-metal units [Ag_4O_4] connect alternatively through two Ag1–O1 and one Ag1⋯Ag1 interaction into one-dimensional wave-like [–Ag–O–] chain along *a* axis (Fig. 3b). Simultaneously, a one-dimensional zig–zag Ag(I) chain hide in the [–Ag–O–] chain based on Ag⋯Ag interactions. The [–Ag–O–] chains are interlaced by 1,2-ethylenediphosphonate groups into a three-dimensional zeolite-like framework with one-dimensional ellipse-like channels along *a* axis (Fig. 1c). The ellipse channels are occupied by ethylene groups. While the zig–zag Ag(I) chains are connected by Ag1⋯Ag2 into a three-dimensional Ag⋯Ag interacted substructural net (Fig. 3d).

Compound **1** has one-dimensional channels, which is similar to zeolite. The structure of **1** is obviously different from the common pillar-like structures of metal organodiphosphonates in following two aspects [10–28]: (1) In the structure **1** there is a three-dimensional Ag–O with one-dimensional channels, while there are two-dimensional metal-oxygen layers in pillar-like structure. (2) Organodiphosphonate groups are inclused in the channel, but in common pillar-like structure the organodiphosphnate groups lie between two metal-oxygen layer.

3.3. Electrical property

The impedance ($-Z''$ vs. Z') curves at each temperature in the range of 50–170 °C are composed of only one arc, respectively, due to the response of the grain interior [42]. The conductivities at each of the temperatures have been calculated based on the intercept of low frequencies of the arcs with the real Z'-axis, respectively. The grain interior conductivity of the compound as a function of reciprocal temperatures ($1000/T$) with increasing and decreasing temperature processes are showed in Fig. 4. The result of temperature increasing process almost coincides with that of temperature decreasing process. And each curve shows only one linear dependency.

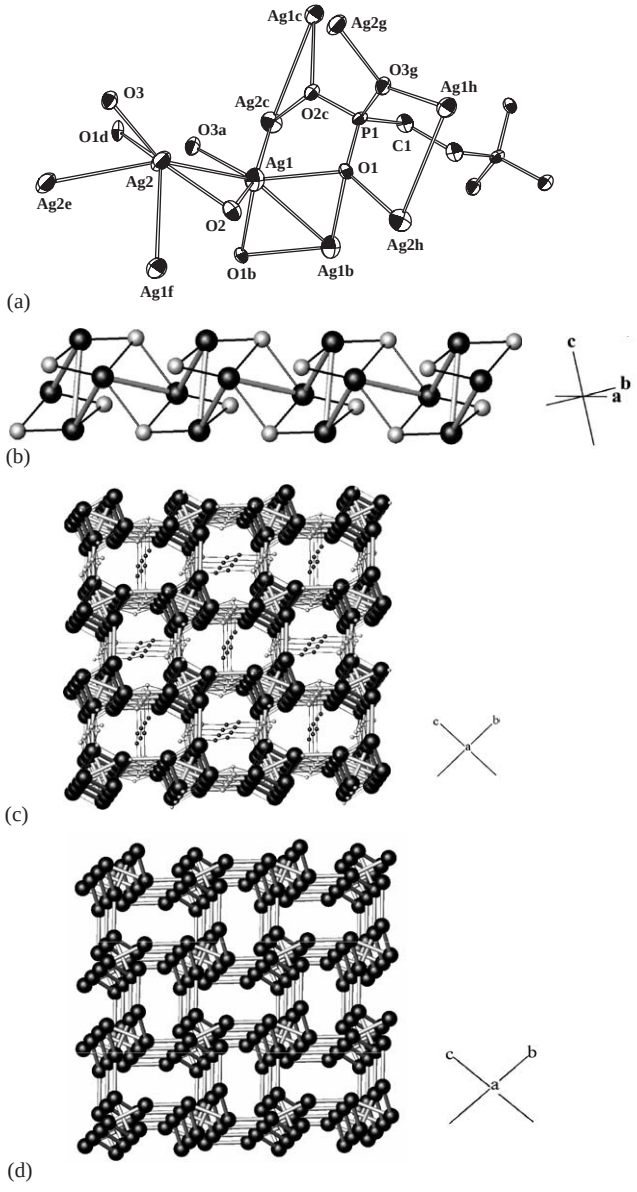

Fig. 3. (a) ORTEP view of **1** shows the coordination geometries of silver and phosphorus (ellipsoids at 50% probability). Hydrogen atoms are omitted for clarity. Symmetry code: (a) $1/2-x,-1/2+y,-3/2-z$; (b) $-x,-1-y,-1-z$; (c) $1/2+x.-1/2-y,1/2+z$; (d) $1/2+x,-1/2-y,-1/2+z$; (e) $-x,-y,-2-z$; (f) $-1/2+x,-1/2-y,-1/2+z$; (g) $-x,-y,-1-z$; (h) $-1/2+x,-1/2-y,1/2+z$. Selected bond lengths (Å) and bond angles (°): Ag1–O1 = 2.390(11), Ag1–O2 = 2.305(12), Ag1–O3*a* = 2.334(12), Ag1–O1*b* = 2.530(10), Ag2–O2 = 2.203(12), Ag2–O3 = 2.301(12), Ag2–O1*d* = 2.380(11), Ag1–Ag1*b* = 3.063(3), Ag1–Ag2 = 3.214(2), Ag1–Ag2*c* = 3.223(2), Ag2–Ag2*e* = 3.173(3), O2–Ag1–O3*a* = 119.6(4), O2–Ag1–O1 = 105.4(4), O3*a*–Ag1–O1 = 132.6(4), O2–Ag1–O1*b* = 103.2(4), O3*a*–Ag1–O1*b* = 81.8(4), O1–Ag1–O1*b* = 103.0(3), O2–Ag2–O3 = 145.4(4), O2–Ag2–O1*d* = 126.4(4), O3–Ag2–O1*d* = 85.8(4). (b) View of the {–Ag–O–} chain; (c) pack view of the zeolite-like framework. (d) Pack view of the three-dimensional Ag···Ag interacted substructural net. Fig. 3(b)–(d): Ag, P, O and C atoms are represented in big black, medium gray, small gray and small black balls, respectively. Thick gray lines indicate Ag···Ag interactions. Hydrogen atoms and not related atoms are omitted for clarity.

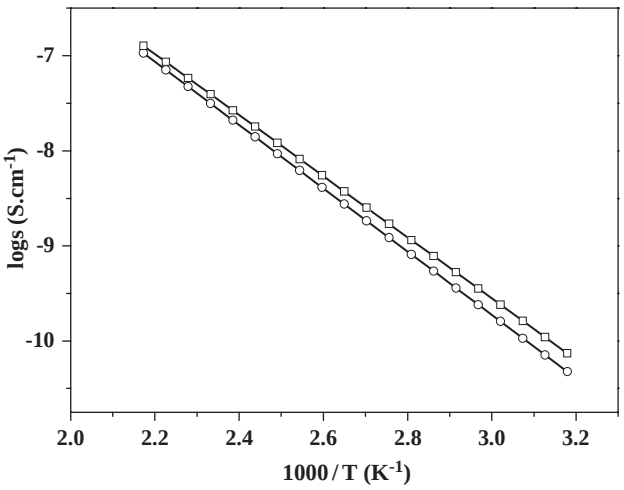

Fig. 4. Conductivity (σ) versus reciprocal temperature of **1** with temperature increasing (○) and decreasing processes (□).

According to the definition of Kittel [43], the conductivity of semiconductors is 10^{-9}–$10^{2}\,S\,cm^{-1}$, in the temperature range of 100–170 °C **1** belongs to semiconductor. The activation energies associated with the grain interior conductivity is 0.70 and 0.67 eV based on temperature increasing and decreasing processes, respectively. At 170 °C the maximum conductivities reached to 6.5×10^{-7} and $7.3\times10^{-7}\,S\,cm^{-1}$ according to temperature increasing and decreasing processes, respectively.

3.4. Electric band structure

Electric band-structure calculations are preformed for **1** by using the formalism of the extended Hückel theory (EHT) crystal orbital method [44,45]. X-ray crystallographic data are used to describe the unit cell. For the semiempirical calculations, only the outer valence orbitals are adopted for all atoms, as shown in Table 2. The parameters, ionization energy H_{ii} and STO exponents ξ for Ag, O, P, C and H atoms used in the EHT calculations are also given in Table 2, which are kept constant. As shown in Fig. 5, its energy gap is 3.28 eV, which is also in the range of the semiconductors. Ag 4*d* electrons bands are dominatingly lying in the district 1.3–3.1 eV lower than Fermi level (−12.28 eV), while the ones consisted of its 5*p* orbitals are mainly 6.8 eV higher than Fermi level. The characterizations of the top of valence-bands are two degenerate π antibonding bands between O 2*p* and P 3*p* orbitals of $-PO_3$ group, whereas the bottom of conductor-bands are mainly the antibonding bands between Ag 5*s* and O 2*p* orbital and the bond bands among Ag 5*s* orbitals. Therefore, under the thermal or optical excitation, the conductivity of **1** is mainly due to the transfer of π aitibonding electrons of $-PO_3$ group through O atom to Ag 5*s* orbital, which leads to the electrons hold on Ag–O

Table 2
The parameters H_{ii} and ξ for extended Hückel calculations (when two exponents are used the corresponding coefficients are given in parentheses)

Orbital	Ag 5*s*	Ag 5*p*	Ag 4*d*	O 2*s*	O 2*p*	P 3*s*	P 3*p*	C 2*s*	C 2*p*	H 1*s*
H_{ii}	11.10	5.80	14.50	32.30	14.80	18.60	14.00	21.40	11.40	13.60
ξ_1	2.244	2.202	6.070 (0.5591)	2.275	2.275	1.750	1.300	1.625	1.625	1.300
ξ_2			2.663 (0.6047)							

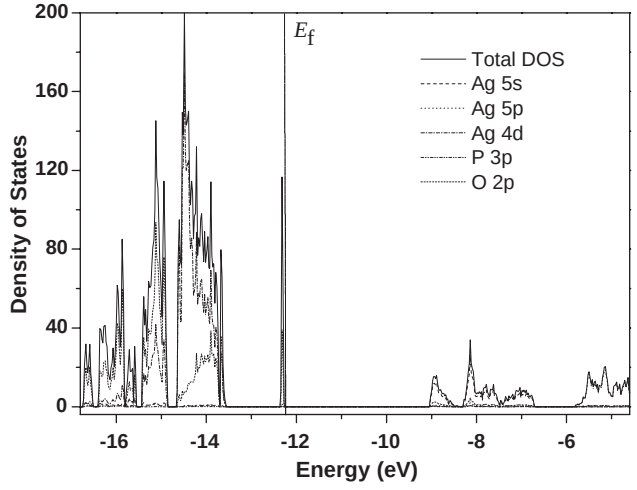

Fig. 5. Density of states for **1** with the projected Ag, P and O dominating orbital contributions.

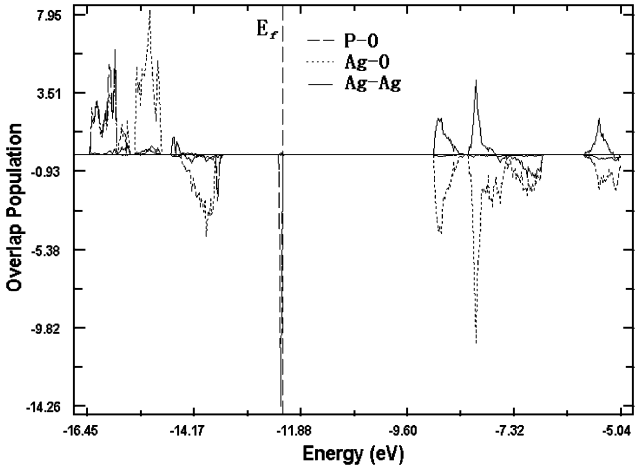

Fig. 6. P–O, Ag–O and Ag–Ag bond overlap populations (COOP) for **1** as a function of energy. As usual, a positive value indicates a bonding interaction.

σ antibonding bands and Ag–Ag bonding ones. After magnifying the −17.25 to 0.40 eV region of the density of states (DOS) plot, it can be seen that DOS of Ag 4*d*, 5*s* and 5*p* are actually full of this region. It is due to the mixing of high energy *s* and *p* functions into predominantly *d*-type molecular orbitals that the Ag–Ag antibonding component in silver *d*-band region is depressed, which results in the replacement of closed-shell $d^{10}-d^{10}$ repulsive interactions by weakly bonding interactions [46–50]. As shown in Fig. 6, the strength of Ag⋯Ag interaction is much smaller than that of P⋯O and Ag⋯O interactions under Fermi level. As excitated, electrons transfer to Ag–O antibonding bands and the strong Ag⋯Ag interaction bonding bands over Fermi level. The compound's Ag–O bond and Ag⋯Ag interaction are weakened and enhanced, respectively, which favors to promote the formation of the three-dimensional Ag⋯Ag bonded substructural net shown in Fig. 3(d). This substructure which exists in many silver compounds [50] is to further improve the conductivity of **1**. Just as the formation of the Ag⋯Ag interacted substructure, **1** bear the semiconductor character under excitation, which is in good agreement with its conductivity and structural characteristic.

4. Conclusion

In conclusion, we have described the syntheses, structure characterization and electric property of the new silver organodiphosphonate $[Ag_4(O_3PCH_2CH_2PO_3)]$ **1**. The structure is a zeolite-like three-dimensional structure with one-dimensional channels containing ethylene groups and a three-dimensional Ag⋯Ag interacted substructural net. The grain interior conductivity of **1** increases continuously with temperature rising in the range of 50–170 °C. From EHT calculations, it is shown that under the thermal or optical excitation, the conductivity of **1** is mainly due to the transfer of π antibonding electrons of $-PO_3$ group through O atom to Ag 5*s* orbital, which also leads to the enhancement of Ag⋯Ag interaction and prompts the formation of the Ag⋯Ag bonded substructural net.

Acknowledgments

This research was supported by grants from the State Key Laboratory of Structure Chemistry, Fujian Institute of Research on the Structure of Matter, the National Ministry of Science and Technology of China (001CB1089), Chinese Academy of Sciences (CAS), the National Science Foundation of China (20273073, 20333070 and 90206040), the Science Foundation of CAS (2002F014) and Fujian Province for research

funding support (2002J007, 2003J042, 2004J041 and 2004J042). Xiang gratefully acknowledges the support of K.C. Wong Education Foundation, Hong Kong.

References

[1] L.C. Brousseau III, T.E. Mallouk, Anal. Chem. 69 (1997) 679–687.
[2] L.C. Brousseau III, D.J. Aurentz, A.J. Benesi, T.E. Mallouk, Anal. Chem. 69 (1997) 688–694.
[3] F. Odobel, B. Bujoli, D. Massiot, Chem. Mater. 13 (2001) 163–173.
[4] H. Byrd, A. Clearfield, D. Poojary, K.P. Reis, M.E. Thompson, Chem. Mater. 8 (1996) 2239–2246.
[5] T.E. Mallouk, J.A. Gavin, Acc. Chem. Res. 31 (1998) 209–217.
[6] A. Clearfield, Chem. Mater. 10 (1998) 2801–2810.
[7] G. Alberti, U. Costantino, F. Marmottini, R. Vivani, P. Zappelli, Angew. Chem. Int. Ed. 32 (1993) 1357–1359.
[8] G. Alberti, F. Marmottini, S. Murcia, R. Vivani, Angew. Chem. Int. Ed. 33 (1993) 1594–1597.
[9] J.E. Haskouri, C. Guillem, J. Latorre, A. Beltrán, D. Beltrán, P. Amorós, Eur. J. Inorg. Chem. (2004) 1804–1807.
[10] C. Bellitto, F. Federici, Chem. Mater. 10 (1998) 1076–1082.
[11] D.M. Poojary, B. Zhang, A. Clearfield, J. Am. Chem. Soc. 119 (1997) 12550–12559.
[12] K. Barthelet, M. Nogues, D. Riou, G. Férey, Chem. Mater. 14 (2002) 4910–4918.
[13] D.M. Poojary, B. Zhang, P. Bellinghausen, A. Clearfield, Inorg. Chem. 35 (1996) 4942–4949.
[14] D.I. Arnold, X. Ouyang, A. Clearfield, Chem. Mater. 14 (2002) 2020–2027.
[15] D.M. Poojary, B. Zhang, A. Clearfield, Chem. Mater. 11 (1999) 421–426.
[16] B. Zhang, D.M. Poojary, A. Clearfield, Inorg. Chem. 37 (1998) 1844–1852.
[17] D.M. Poojary, B. Zhang, P. Bellinghausen, A. Clearfield, Inorg. Chem. 35 (1996) 5254–5263.
[18] H.G. Harvey, J. Hu, M.P. Attfield, Chem. Mater. 15 (2003) 179–188.
[19] M. Bujoli-Doeuff, M. Evain, P. Janvier, D. Massiot, A. Clearfield, Z. Gan, B. Bujoli, Inorg. Chem. 40 (2001) 6694–6698.
[20] F. Serpaggi, G. Férey, J. Mater. Chem. 8 (1998) 2749–2755.
[21] C. Serre, G. Férey, Inorg. Chem. 38 (1999) 5370–5373.
[22] C. Serre, G. Férey, Inorg. Chem. 40 (2001) 5350–5353.
[23] G. Alberti, R. Vivani, S.M. Mascarós, J. Mol. Struct. 471 (1998) 81–92.
[24] G. Alberti, U. Costantino, F. Marmottini, R. Vivani, P. Zappelli, Angew. Chem. Int. Ed. 32 (1993) 1357–1359.
[25] G. Alberti, F. Marmottini, S. Murcia, R. Vivani, Angew. Chem. Int. Ed. 33 (1993) 1594–1597.
[26] G. Alberti, S. Murcia, R. Vivani, Mater. Chem. Phys. 35 (1993) 187–192.
[27] M.B. Diness, R.E. Cmksey, P.C. Griffith, R.H. Lane, Inorg. Chem. 22 (1983) 1003–1004.
[28] M.B. Dines, P.C. Griffith, Polyhedron 2 (1983) 607–611.
[29] D.S. Sagatys, C. Dahlgren, G. Smith, R.C. Bott, J.M. White, J. Chem. Soc., Dalton Trans. (2000) 3404–3410.
[30] T.G. Appleton, K.A. Byriel, J.R. Hall, C.H.L. Kennard, D.E. Lynch, J.A. Sinkinson, G. Smith, Inorg. Chem. 33 (1994) 444–455.
[31] O.S. Jung, Y.J. Kim, Y.A. Lee, S.W. Kang, S.N. Choi, Cryst. Growth Design 4 (2004) 23–24.
[32] S. Ganguly, S. Chattopadhyay, C. Sinha, A. Chakravorty, Inorg. Chem. 39 (2000) 2954–2956.
[33] E. Bosch, C.L. Barnes, Inorg. Chem. 41 (2002) 2543–2547.
[34] P. Pyykkö, Chem. Rev. 97 (1997) 567–636.
[35] K. Singh, J.R. Long, P. Stavropoulos, J. Am. Chem. Soc. 119 (1997) 2942–2943.
[36] Q.M. Wang, T.C.W. Mak, J. Am. Chem. Soc. 123 (2001) 7594–7600.
[37] S.L. Zheng, J.P. Zhang, W.T. Wong, X.M. Chen, J. Am. Chem. Soc. 125 (2003) 6882–6883.
[38] A.K. Bhattacharya, G. Thyagarajan, Chem. Rev. 81 (1981) 415–430.
[39] K. Moedritzer, R.R. Irani, J. Inorg. Nucl. Chem. 22 (1961) 297–304.
[40] G.M. Sheldrick, SHELXT 97, Program for Crystal Structure Refinement, University of Göttingen, Germany, 1997.
[41] A. Bondi, J. Phys. Chem. 68 (1964) 441–451.
[42] E. Vila, J.M. Rojo, J.E. Iglesias, A. Castro, Chem. Mater. 16 (2004) 1732–1739.
[43] C. Kittel, Solid State Physics, first ed., Wiley, New York, 1976.
[44] M.H. Whangbo, R. Hoffmann, J. Am. Chem. Soc. 100 (1978) 6093–6098.
[45] J. Ren, W. Liang, M.H. Whangbo, CAESAR Version 2.0, PrimeColor Software, Inc., 1998.
[46] P.K. Mehrotra, R. Hoffmann, Inorg. Chem. 17 (1978) 2187–2189.
[47] A. Dedieu, R. Hoffmann, J. Am. Chem. Soc. 100 (1978) 2074–2079.
[48] Y. Jiang, S. Alvarez, R. Hoffmann, Inorg. Chem. 24 (1985) 749–757.
[49] C.X. Cui, M. Kertesz, Inorg. Chem. 29 (1990) 2568–2575.
[50] T.D. Brennant, J.K. Burdett, Inorg. Chem. 33 (1994) 4794–4799.